Prediction of Berreman-like magnon-polariton modes in antiferromagnetic films

1998 J. Phys.: Condens. Matter 10 7809

(http://iopscience.iop.org/0953-8984/10/35/013)

J. Phys.: Condens. Matter **10** (1998) 7809–7822. Printed in the UK PII: S0953-8984(98)90520-3

Prediction of Berreman-like magnon–polariton modes in antiferromagnetic films

Thomas Dumelow

Departamento de Física, Universidade Federal do Rio Grande do Norte, 59072-970 Natal RN, Brazil

Received 9 January 1998, in final form 29 April 1998

Abstract. We consider the surface polaritons at the interface of an antiferromagnet with a metal, predict the effect of such modes on the far-infrared spectrum of an antiferromagnetic film deposited on a metal, and discuss how they may be used to aid the detection of magnon features experimentally. We examine the particular example of an FeF_2 film deposited on a metal substrate. This type of structure may be used to represent many ferromagnet/antiferromagnet bilayer systems, since the ferromagnetic layers of such systems are frequently metallic and, furthermore, do not contribute to the far-infrared magnon spectrum. The associated surface polaritons are unusual for a number of reasons. Firstly, they extend down to zero wavevector, so, in contrast to most surface polariton modes, they should be observable in simple oblique-incidence reflectivity. Secondly, modes can exist in both s and p polarization. Thirdly, the modes show significant shifts from the simple surface polariton frequencies when the film becomes thin. Fourthly, the p-polarization modes show up strongly even for very thin films. Therefore, by choosing the correct geometry, one should be able to enhance considerably the far-infrared spectral features associated with magnon modes in such films.

1. Introduction

In recent years thin-layer magnetic structures have increasingly grown in importance. A number of experiments on magnons in ferromagnetic layers have been performed, and have shown large deviations from bulk behaviour [1]. Considerably less has been done with thin antiferromagnet layers, partly due to the experimental difficulties involved.

The technique of far-infrared spectroscopy has been successfully used to study magnons in antiferromagnets both in the 1960s and in more recent studies [2–7], and it appears reasonable to consider this technique for studying such modes in antiferromagnetic layers of thin-film structures. However, the free-space wavelength of the appropriate far-infrared radiation is of order 100 μm, whereas the antiferromagnet layer thickness may be of order 10 nm. At first sight, therefore, the prospects for using far-infrared spectroscopy to detect magnons in such a layer do not look promising.

One type of structure of interest is the ferromagnet/antiferromagnet bilayer, the ferromagnetic layer often being metallic [8–10]. In this paper we consider the optics associated with the far-infrared spectroscopy of magnons in the antiferromagnetic layer of such structures, using as our model an antiferromagnetic film deposited on a metallic substrate. We show that, for this type of structure, far-infrared magnon spectra may indeed be observable in antiferromagnetic films of thickness several orders of magnitude less than the wavelength of radiation used in detecting the spectral features.

0953-8984/98/357809+14$19.50

The optics of magnons in thin antiferromagnetic layers deposited on metallic substrates has an interesting analogy in the optics of phonons in films of ionic salts deposited on metallic substrates. The latter study was performed in 1963 by Berreman [11], who measured the p-polarization oblique-incidence reflectivity for a series of alkali halide films on metal substrates, and observed sharp dips at the longitudinal optical (LO) phonon frequencies of the salts. This type of measurement has proved very sensitive, and the principle has since been used as the basis for studying adsorbed species on metal surfaces [12, 13].

A useful way of considering the dips observed in Berreman's experiments is in terms of absorption by surface polariton modes at the salt/metal interface [14, 15]. Usually one can only couple to surface modes using a special geometry, incorporating, for example, an attenuated total reflection (ATR) prism, which enhances the in-plane wavevector component [16]. At frequencies just above those of the LOs, however, dips due to the surface modes at the relevant interface in Berreman's samples should be observed in simple oblique-incidence reflectivity. To a good approximation these dips can be regarded as occurring at the LO frequencies themselves.

Although, due to the finite thickness of the salt layer, the surface mode model acts only as an approximation to the Berreman effect, it has nevertheless served as a useful way of explaining the observed phenomena, and any discrepancy in frequency has been small in practice. It therefore seems reasonable to adopt the same approach in considering the modes expected for a thin antiferromagnetic film on a metal.

In this paper we consider the surface polariton modes at an antiferromagnet/metal interface, and show that such modes can exist in both s and p polarization, in both cases in the wavevector range observable using simple oblique-incidence reflectivity. Interestingly, we find that only the p polarization modes show up strongly in the calculated spectra of antiferromagnetic layers on metals, and that these modes are still evident even in very-thin-film structures. In contrast to the case discussed by Berreman, large shifts from the surface mode frequencies are seen for samples in which the layer is thin.

The plan of the paper is as follows. In section 2 we derive the surface polariton dispersion relationships at an antiferromagnet/metal interface. In section 3 we show numerical calculations of surface mode dispersion curves based on the results of section 2. In section 4 we present explicit calculations of reflectivity spectra for an antiferromagnet film deposited on a metal, and compare the dip frequencies with the surface mode frequencies calculated in section 3. We consider how the spectrum changes when the film is very thin, and the relevance to the experimental observation of magnon features. Finally, conclusions are presented in section 5.

2. Surface polaritons at an antiferromagnet/metal interface

In this section we work out the dispersion relations for surface modes at the boundary of a uniaxial antiferromagnet with a metal. For simplicity, we only consider results in the absence of an applied field. We take layer 1 (the top layer) to be the antiferromagnet, and layer 2 to be the metal. The z-axis is normal to the interface, the positive z-direction being upwards, and we consider surface polaritons propagating along $\boldsymbol{x}$.

Layer 1 (the antiferromagnet) has a dielectric constant ϵ_1, assumed here to be positive. Since the antiferromagnet is uniaxial and there is no external field, the permeability tensor at frequency ω has a component equal to 1 parallel to the anisotropy axis, and components

equal to

$$\mu_\perp = 1 + \frac{8\pi\gamma^2 H_A M_S}{\omega_T^2 - (\omega + \mathrm{i}\Gamma)^2} \tag{1}$$

perpendicular to it [17]. Here γ is the gyromagnetic ratio, H_A the anisotropy field, and M_S the sublattice magnetization. Γ is a damping parameter which we take to be zero for the surface mode dispersion calculation presented in this section. ω_T is the transverse resonance frequency given by

$$\omega_T^2 = \gamma^2(2H_A H_E + H_A^2) \tag{2}$$

with H_E the exchange field. As seen from (1), $\mu_\perp$ has a pole at frequency ω_T. We shall also wish to label a longitudinal frequency ω_L at the zero in $\mu_\perp$. This frequency is given by

$$\omega_L^2 = \omega_T^2 + 8\pi\gamma^2 H_A M_S. \tag{3}$$

We take the anisotropy to be directed along one of the principal axes x, y, or z. In the following discussion we refer to the components μ_{xx}, μ_{yy}, and μ_{zz}. Each of these components takes on a value of either 1 or $\mu_\perp$ according to the anisotropy direction.

Layer 2 (the metal) has a dielectric function ϵ_2 and a permeability constant of 1. Thus the possible ferromagnetic properties of the metal are ignored, since any associated magnons are likely to be at much lower frequencies than those of the antiferromagnet. In calculating the surface mode dispersion we take ϵ_2 to be real and negative.

We consider the case of a real in-plane wavevector of q_x, which will be the same in both layers. The z-component of the wavevector in layer 1 depends on the plane of polarization, and is given by

$$q_{1z} = \left(\frac{\omega^2}{c^2}\epsilon_1\mu_{xx} - \frac{\mu_{xx}}{\mu_{zz}}q_x^2\right)^{1/2}: \qquad \text{s polarization} \tag{4a}$$

$$q_{1z} = \left(\frac{\omega^2}{c^2}\epsilon_1\mu_{yy} - q_x^2\right)^{1/2}: \qquad \text{p polarization.} \tag{4b}$$

In layer 2 the z-component of the wavevector is given by

$$q_{2z} = \left(\frac{\omega^2}{c^2}\epsilon_2 - q_x^2\right)^{1/2}. \tag{5}$$

For surface polaritons to exist, the field amplitudes should decay exponentially away from the interface in each of the two layers, both of which we consider to be semi-infinite. Thus the field varies as $\exp(\mathrm{i}q_{1z}z)$ in layer 1, and $\exp(-\mathrm{i}q_{2z}z)$ in layer 2, with both q_{1z} and q_{2z} imaginary. The condition that q_{2z} is imaginary is automatically satisfied from (5) because $\epsilon_2 < 0$, but in order to have q_{1z} imaginary one must satisfy the inequality

$$\frac{\mu_{xx}}{\mu_{zz}}q_x^2 > \frac{\omega^2}{c^2}\epsilon_1\mu_{xx}: \qquad \text{s polarization} \tag{6a}$$

$$q_x^2 > \frac{\omega^2}{c^2}\epsilon_1\mu_{yy}: \qquad \text{p polarization.} \tag{6b}$$

At the interface, the tangential components of the $\boldsymbol{E}$- and $\boldsymbol{H}$-fields must be continuous. This condition, combined with the localization requirement that the fields vary as $\exp(\mathrm{i}q_{1z}z)$ in layer 1 and $\exp(-\mathrm{i}q_{2z}z)$ in layer 2, leads to the surface polariton relation

$$\frac{q_{1z}}{\mu_{xx}} + q_{2z} = 0: \qquad \text{s polarization} \tag{7a}$$

$$\frac{q_{1z}}{\epsilon_1} + \frac{q_{2z}}{\epsilon_2} = 0: \qquad \text{p polarization.} \tag{7b}$$

Since we have defined q_{1z} and q_{2z} in such a way that they are both positive imaginary quantities, it follows that

$$\mu_{xx} < 0: \qquad \text{s polarization} \tag{8a}$$

$$\epsilon_1\epsilon_2 < 0: \qquad \text{p polarization.} \tag{8b}$$

Finally, we make equation (7) more manageable by substituting for q_{1z} and q_{2z} from equations (4) and (5) and rearranging, so that we get a simple dispersion relation in terms of q_x:

$$q_x^2 = \frac{\omega^2}{c^2}\frac{\epsilon_2\mu_{xx} - \epsilon_1}{\mu_{xx} - 1/\mu_{zz}}: \qquad \text{s polarization} \tag{9a}$$

$$q_x^2 = \frac{\omega^2}{c^2}\frac{\epsilon_1 - \epsilon_2\mu_{yy}}{\epsilon_1/\epsilon_2 - \epsilon_2/\epsilon_1}: \qquad \text{p polarization.} \tag{9b}$$

We expect surface polaritons to occur at frequencies at which equation (9) is satisfied simultaneously with the inequalities in equations (8) and (6). Furthermore, we are only interested in real q_x-values, so solutions only exist when the right-hand side of equation (9) is positive. We now examine the implications of equations (8) and (6).

Equation (8) imposes restrictions on the signs of the dielectric functions or permeability tensor components for which surface modes can occur. In s polarization, surface modes are only possible for μ_{xx} negative, as seen in (8*a*). Thus, for uniaxial antiferromagnets of the type considered here, such modes can only exist if the anisotropy is along $\boldsymbol{y}$ or $\boldsymbol{z}$ and if the frequency falls in the range $\omega_T < \omega < \omega_L$. In p polarization, however, equation (8*b*) is automatically satisfied in the system considered here, and there is no restriction on the sign of any of the permeability tensor components.

Equation (6) only allows the presence of surface modes if q_x is greater than (or less than) a certain value. Conventional surface polariton studies have concentrated on modes at an interface between an optically active medium and a vacuum. The equivalent equation in such cases is $q_x > \omega/c$. Experimentally, this condition cannot be met in simple reflectivity from vacuum, and a special geometry, such as that used in ATR studies, is required [16]. In the case considered in this paper, however, we shall find that equation (6) does not impose such restrictions.

In considering the allowed q_x-range for surface polaritons in s polarization, it is worth noting that (6*a*) is only of relevance in regions where (8*a*) is satisfied. In such regions, we may simplify (6*a*) to

$$\frac{q_x^2}{\mu_{zz}} < \frac{\omega^2}{c^2}\epsilon_1: \qquad \text{s polarization.} \tag{10}$$

Since we are considering the case of ϵ_1 positive, we thus see that there is no restriction on q_x wherever μ_{zz} (as well as μ_{xx}) is negative. Furthermore, if μ_{zz} is positive and μ_{xx} negative, comparison of (10) with (9*a*) shows that (10) is always satisfied. Therefore, wherever (8*a*) is satisfied, so is (6*a*).

In p polarization, equation (6*b*) shows that there is no restriction on q_x in the frequency region for which μ_{yy} is negative ($\omega_T < \omega < \omega_L$ with anisotropy along either $\boldsymbol{x}$ or $\boldsymbol{z}$). Furthermore, comparison of equations (6*b*) and (9*b*) shows that even if μ_{yy} is positive, equation (6*b*) is always satisfied where q_x is real.

Thus, from the above, we see that, in practice, the inequalities in (8) and (6) impose no restrictions on either the q_x-range or the sign of the permeability tensor components in either polarization, other than that μ_{xx} must be negative in s polarization. Surface modes may therefore exist in both s and p polarization and, since there is no restriction

on the wavevector component q_x, may extend all the way down to $q_x = 0$, at a frequency corresponding to $\mu_{xx} = \epsilon_1/\epsilon_2$ in s polarization and $\mu_{yy} = \epsilon_1/\epsilon_2$ in p polarization. It follows that it should be possible to couple to the surface modes of an antiferromagnet/metal system without the need of a special geometry such as that of ATR. The modes should thus be observable in simple oblique-incidence reflectivity from vacuum, and we show examples of this in section 4.

3. Calculated dispersion curves

We now consider specific examples illustrating the principles outlined above. We use numbers appropriate for FeF_2 in contact with a metal. For the purpose of calculating dispersion curves, both layers are considered to be semi-infinite.

For the antiferromagnetic film, we use the same parameters as applied for recent 4.2 K experimental studies [5–7]: $\epsilon_1 = 5.5$, $M_S = 0.056$ T, $H_A = 19.745$ T, $H_E = 53.313$ T, and $\gamma = 1.05$ cm^{-1} T^{-1}, corresponding to a transverse resonance frequency of $\omega_T = 52.45$ cm^{-1}. In calculating dispersion curves corresponding to equation (9) we set the damping parameter Γ equal to zero, although we shall give it a finite value for reflectivity calculations in the following section.

The dielectric function of the metal is represented by a simple Drude expression of the form

$$\epsilon_2 = 1 - \frac{\omega_p^2}{\omega^2 + \mathrm{i}\omega\Gamma_p} \tag{11}$$

where ω_p is the plasma frequency and Γ_p a corresponding plasma damping term. A simple Drude model for iron would give a plasma frequency of about 120 000 cm^{-1}, corresponding to a free-electron density of 1.7×10^{29} m^{-3} [18]. In the work presented here, we use this value for the plasma frequency, and compare the results with those for a hypothetical metal having a much lower plasma frequency of 150 cm^{-1}. In the frequency range of interest, the corresponding dielectric functions in layer 2 are about -5.2×10^6 for $\omega_p = 120\,000$ cm^{-1} and -7.2 for $\omega_p = 150$ cm^{-1}. We set the plasma damping term Γ_p equal to zero for the dispersion curve calculations.

In figure 1, we show the dispersion curves corresponding to equation (9) in different situations. On each graph, surface mode dispersion curves are shown both for $\omega_p = 150$ cm^{-1} and for $\omega_p = 120\,000$ cm^{-1}. The bulk regions of the antiferromagnet layer are also indicated. In these regions, q_{1z} is real, i.e., equation (6) is not satisfied.

Figures 1(a) and 1(b) show the s-polarization dispersion curves when the anisotropy is along $\boldsymbol{y}$ ($\mu_{yy} = 1$ and $\mu_{xx} = \mu_{zz} = \mu_\perp$) and $\boldsymbol{z}$ ($\mu_{zz} = 1$ and $\mu_{xx} = \mu_{yy} = \mu_\perp$) respectively. We see that, for each of the two plasma frequencies modelled, a surface mode occurs in the region $\omega_T < \omega < \omega_L$, as might be expected from (8*a*). In each case the mode extends down to $q_x = 0$ at the frequency at which $\mu_\perp = \epsilon_1/\epsilon_2$. In the case of $\omega_p = 120\,000$ cm^{-1}, this occurs at a frequency that cannot, in practice, be resolved from ω_L itself. In figure 1(a), the surface mode is real, extending to $q_x \to \infty$ at a frequency

$$\omega_s = \left(\omega_T^2 + 4\pi\gamma^2 H_A M_S\right)^{1/2}$$

corresponding to $\mu_\perp = -1$. In figure 1(b), however, the surface mode is virtual, terminating at a finite q_x-value at frequency ω_L.

There are no s-polarized modes for anisotropy along $\boldsymbol{x}$. This is because $\mu_{xx} = 1$ everywhere, so (8*a*) is never satisfied.

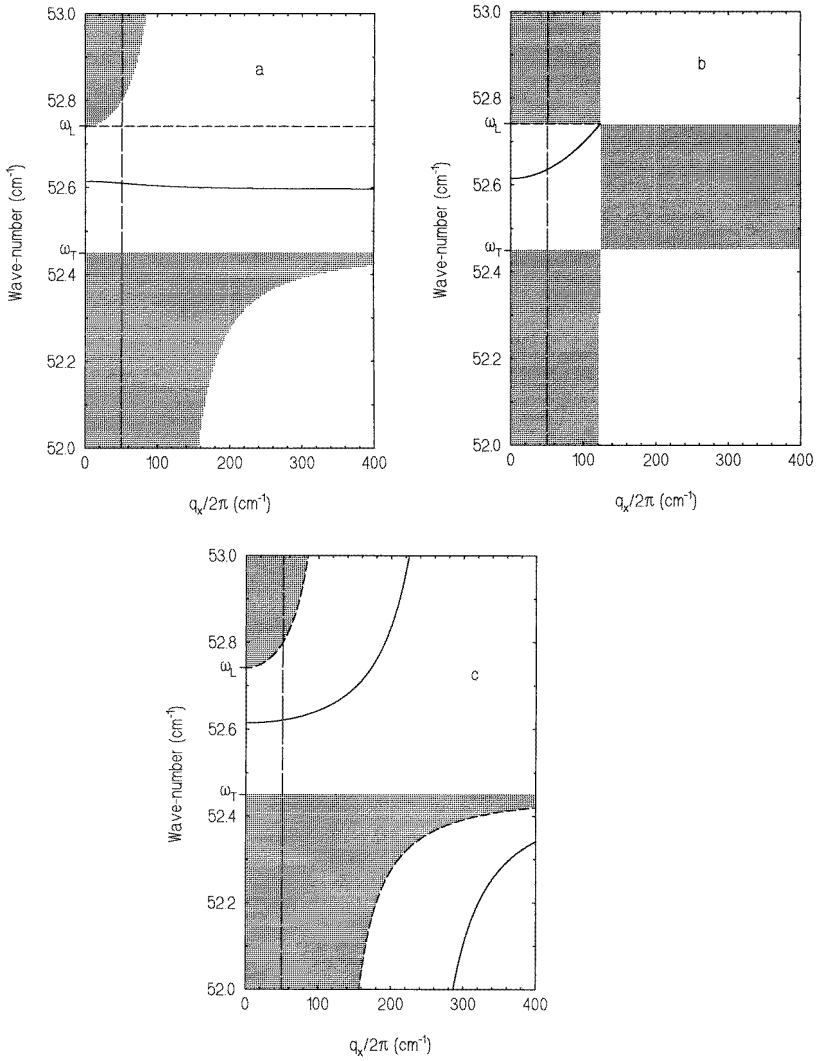

Figure 1. Dispersion curves for surface polaritons at the interface between FeF_2 and a metal with plasma frequency ω_p equal to either 150 cm^{-1} (solid lines) or 120 000 cm^{-1} (dashed lines). (a) s polarization, anisotropy along $\boldsymbol{y}$, (b) s polarization, anisotropy along $\boldsymbol{z}$, (c) p polarization, anisotropy along $\boldsymbol{x}$ or $\boldsymbol{z}$. Shaded areas indicate bulk regions of the antiferromagnet (i.e., regions in which equation (6) is not satisfied). The near-vertical dashed lines are scan lines corresponding to an angle of incidence of 75°. Note that in (b) and (c) the $\omega_p = 120\,000$ cm^{-1} curves fall at the edge of bulk regions.

Figure 1(c) shows p-polarized dispersion curves for anisotropy along either $\boldsymbol{x}$ or $\boldsymbol{z}$. The results are identical because $\mu_{yy} = \mu_\perp$ in both cases, and is the only permeability tensor component that enters the calculations. For anisotropy along $\boldsymbol{y}$, however, $\mu_{yy} = 1$, so there will be no magnetic contribution to any modes in such a geometry. We therefore restrict our discussion of p-polarization modes to the two geometries represented in figure 1(c). As in the s-polarization cases, there is a mode extending down to $q_x = 0$ at a frequency corresponding to $\mu_\perp = \epsilon_1/\epsilon_2$. However, in this case, the mode is not restricted to frequencies for which

$\mu_\perp$ is negative, and extends above ω_L. In addition to this mode, we see that, at higher q_x-values, there is also a lower-frequency branch extending to $q_x \to \infty$ at ω_T.

4. Reflectivity calculations

Since the surface modes considered in the above sections extend down to $q_x = 0$, we expect simple oblique-incidence reflectivity spectra from vacuum off suitable thin-film structures to include contributions from these surface modes. We have therefore calculated such spectra for a number of antiferromagnet/metal structures, each consisting of an FeF_2 film deposited on a semi-infinite metal. The method of calculation is described elsewhere, and involves the use of standard transfer-matrix techniques [19, 20]. Note that, assuming that the dielectric and permeability functions are correct, the reflectivity calculations are exact. This contrasts with the dispersion curve calculations in the previous section, which for thin-film structures are approximations, since they assume semi-infinite layers.

Figure 2 shows calculated spectra for varying thicknesses, in the range 0.02 to 45 μm, of FeF_2 film deposited on a semi-infinite metal having a plasma frequency ω_p of 150 cm^{-1}. We have included damping parameters of $\Gamma = 0.05$ cm^{-1} for the magnon damping [5–7] in FeF_2 and a small plasma damping of $\Gamma_p = 4$ cm^{-1} in the metal.

For each spectrum, the plot has been divided into three regions, each marked as either a bulk or surface mode region. In the bulk mode regions, ignoring damping, q_{1z} is real, corresponding to the shaded regions of figure 1, whereas in the surface mode region q_{1z} is imaginary. Therefore, ignoring any mixing of modes due to damping, surface modes are forbidden in the bulk mode regions and bulk modes are forbidden in the surface mode region.

In practice the modes in the bulk region are best described as interference modes, since radiation will be reflected both from the vacuum/antiferromagnet interface and from the antiferromagnet/metal interface. The overall reflectivity thus depends on the interference between the reflected partial rays.

In the surface mode region the incident radiation should induce an evanescent field decaying away from the upper interface, i.e., the vacuum/antiferromagnet interface. This field should interact with the surface polariton field decaying away from the layer's lower interface, i.e., the antiferromagnet/metal interface. In the presence of damping mechanisms, this should result in a dip in the spectrum at the surface mode frequency. The overall mechanism is analogous to that which produces surface mode dips in ATR experiments.

The surface mode frequency, as determined from equation (9), should occur where the surface mode dispersion curves intersect with a q_x-value determined in the incident (vacuum) layer:

$$q_x = \frac{\omega}{c} \sin\theta \tag{12}$$

where θ is the angle of incidence from vacuum. The line represented by (12) for $\theta = 75^\circ$ is shown in figure 1 as a near-vertical dashed line.

Figures 2(a) and 2(b) show the s-polarization reflectivity spectra for anisotropy along $\boldsymbol{y}$ and $\boldsymbol{z}$ respectively. We concentrate on two features of these spectra.

Firstly, there are the interference mode dips in the bulk mode region below ω_T. As the film gets thinner, they reduce to a single dip which approaches ω_T.

Secondly, if the thickness falls within a certain range, a dip is also present in the surface mode region. This corresponds to the surface polariton discussed in the previous sections. When the film is too thick, the coupling is weak, and the mode is not seen

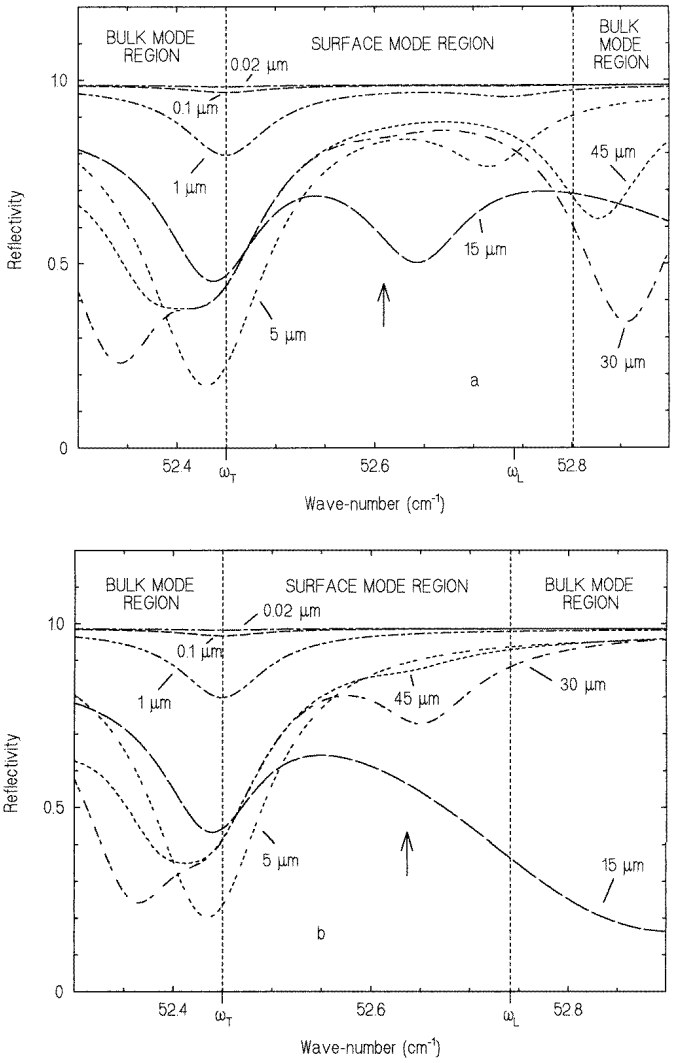

Figure 2. Calculated 75° oblique-incidence reflectivity spectra off various thicknesses of FeF_2 film deposited on a metal with $\omega_p = 150$ cm^{-1} and $\Gamma_p = 4$ cm^{-1}. (a) s polarization, anisotropy along $\boldsymbol{y}$, (b) s polarization, anisotropy along $\boldsymbol{z}$, (c) p polarization, anisotropy along $\boldsymbol{x}$ or $\boldsymbol{z}$. In each case, a vertical arrow indicates the calculated surface polariton frequency at the FeF_2/metal interface.

clearly. Nevertheless, it is clearly seen in the 30 μm spectrum of figure 2(a) and the 45 μm spectrum of figure 2(b), and in both cases its frequency agrees well with that expected from equation (9) (the intersection with the 75° scan line with the appropriate dispersion curve in figure 1), marked by a vertical arrow. For thinner layers, the agreement is not so good, due to the proximity of the antiferromagnet/vacuum interface, and the dip shifts upward in frequency, settling at ω_L in figure 2(a) and merging with a higher-frequency interference feature in figure 2(b).

Figure 2(c) shows the p-polarized spectrum for anisotropy along either $\boldsymbol{x}$ or $\boldsymbol{z}$. As before there are interference features below ω_T as well as the surface mode in the central

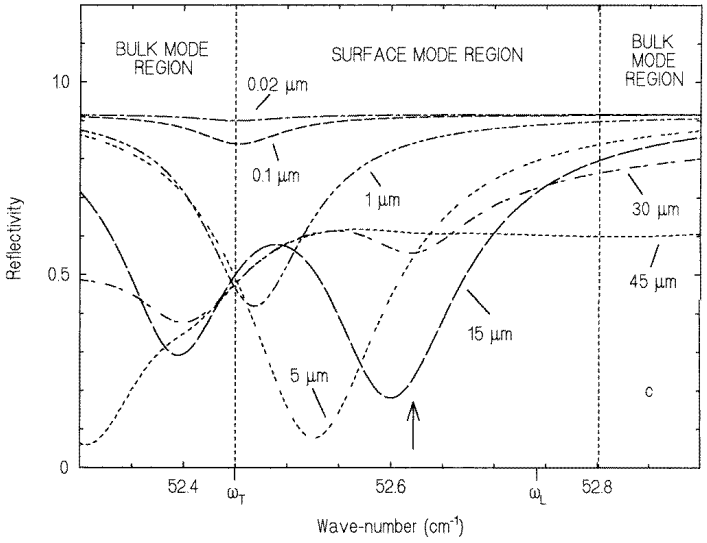

Figure 2. (Continued)

region. According to (9*b*), the surface mode should occur at the frequency marked by a vertical arrow. For a film thickness of 45 μm, a surface mode dip close to the expected frequency can only just be discerned, but at 30 μm it is quite clear. For thinner films, in contrast to the s-polarization results, it shifts downward in frequency towards the pole in $\mu_\perp$ at ω_T eventually merging with the interference dip, but remaining much stronger than the interference dip seen in s polarization.

In figure 3 we examine the results in the case where the substrate is a more typical metal, modelled as having a plasma frequency of 120 000 cm^{-1}. Before examining the spectral features in any detail, we briefly discuss the plasma damping used in the modelling. A plasma damping of $\Gamma_p = 4$ cm^{-1} would roughly correspond to the ideal damping of bulk iron at 10 K in a Drude model [21]. However, since a Drude model may not be ideal for the present regime and since large deviations from the ideal conductivity are likely, especially in thin-film structures, we have performed calculations both with $\Gamma_p = 4$ cm^{-1} and with a much larger damping of $\Gamma_p = 1000$ cm^{-1}. The important qualitative difference between these two cases is that in the former case the dielectric function is predominantly real over the region of interest and in the latter case it is predominantly imaginary. In the s-polarized spectra the results are indistinguishable, and the curves shown in figures 3(a) and 3(b), although calculated for $\Gamma_p = 4$ cm^{-1}, could be used to represent either value of the plasma damping. In the p-polarized spectra (figure 3(c)), a slight difference in the background reflectivity can be observed, so we have drawn two curves for each film thickness. Nevertheless, for p polarization also, the results for the two damping parameters are almost identical. We also find that the exact value of the plasma frequency makes no appreciable difference so long as it is large. Thus we see that, in a real metal, the exact form of the dielectric function over the region of interest makes very little difference to any of the spectra.

In the s-polarized spectra of figures 3(a) and 3(b) the surface mode dips are too weak to be observed. As before, vertical arrows show where dips would be expected on the basis of equation (9).

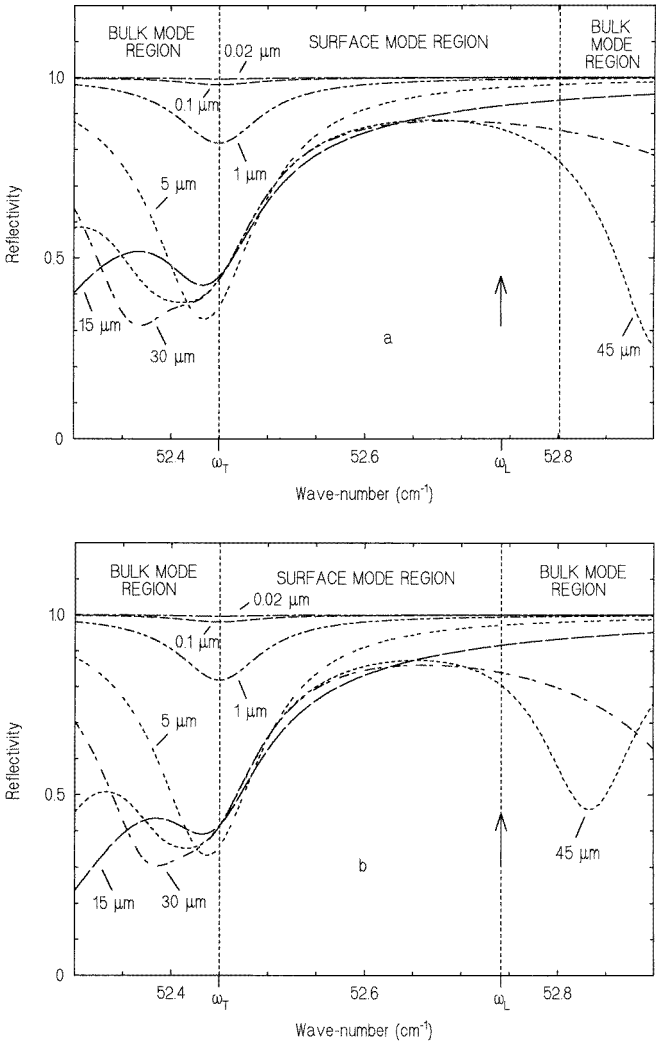

Figure 3. Calculated 75° oblique-incidence reflectivity spectra off various thicknesses of FeF_2 film deposited on a metal with $\omega_p = 120\,000$ cm^{-1}. (a) s polarization, anisotropy along $\boldsymbol{y}$, (b) s polarization, anisotropy along $\boldsymbol{z}$, (c) p polarization, anisotropy along $\boldsymbol{x}$ or $\boldsymbol{z}$. In each case, a vertical arrow indicates the calculated surface polariton frequency at the FeF_2/metal interface. In (a) and (b), the spectra were calculated with $\Gamma_p = 4$ cm^{-1}, but the results with $\Gamma_p = 1000$ cm^{-1} are identical within the plotting resolution. In (c) the results for both values of Γ_p are shown for each value of the thickness (the results for thickness 45μm are identical within the plotting resolution). Where the lines are separated, the upper line corresponds to $\Gamma_p = 4$ cm^{-1} and the lower line to $\Gamma_p = 1000$ cm^{-1}.

In contrast to the s-polarization cases, figure 3(c) shows that p-polarized surface mode dips are still strong if the substrate is highly metallic. For the two thickest films (30 and 45 μm), however, there is no dip visible within the surface mode region, although an interference dip occurs in each case at slightly higher frequency in the bulk region. In fact it is never possible to resolve this feature from the surface mode, suggesting that, for thick films, there is significant mixing between the surface polariton and this interference mode.

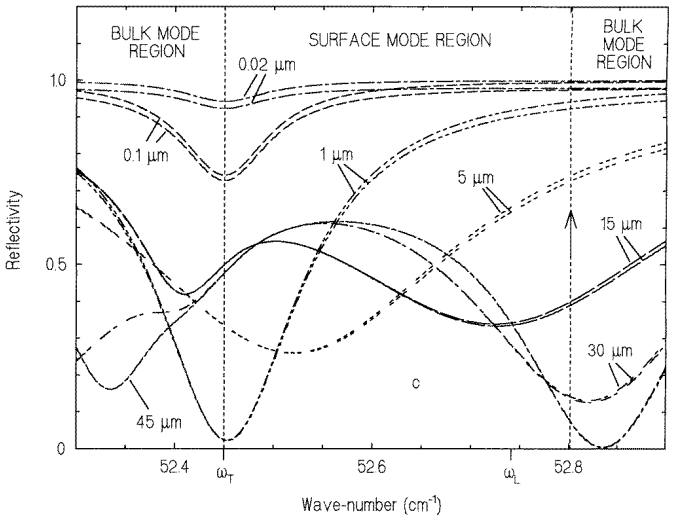

Figure 3. (Continued)

However, for layers thinner than 30 μm, figure 3(c) shows a distinct surface polariton dip, as expected. As before, it shifts to lower frequency as the antiferromagnet film becomes thinner, approaching ω_T. We see that for thin layers the dip in figure 3(c) is even stronger than the corresponding dip in figure 2(c), i.e., the high plasma frequency has enhanced the strength of the dip. Comparison of the s-polarization spectra in figures 3(a) and 3(b) with the p-polarization spectra in figure 3(c) shows that the surface-type p-polarization dips at ω_T can be seen in layers an order of magnitude thinner than can the interference-type s-polarization dips at the same frequency. This result has important experimental implications, suggesting that oblique-incidence p-polarization reflectivity will prove the most sensitive geometry for investigating magnons in this type of structure.

In figure 4 we concentrate on the thinnest-film (0.02 μm) structure, and consider how the p-polarization spectrum is affected by the angle of incidence. For such a thin film, the spectrum can always be considered as a single dip at ω_T. However, the size of this dip is highly dependent on the angle of incidence, and it becomes very large as the incident beam approaches grazing incidence. In gaining the maximum spectral sensitivity, therefore, it appears that one should get as close to this condition as is experimentally feasible.

In order to understand the behaviour for the very thin films it is useful to consider the dips in a different way, considering absorptions in the limit in which there is no field variation across the film thickness [13]. We first consider reflection off a pure metal substrate, then the effect of depositing a thin film onto it. Using field continuity arguments, we carry the appropriate field components in the metal over into the film. Thus, for p polarization, we have E_x, H_y, and D_z continuous. For reflection off a highly metallic substrate, E_x is effectively zero, but H_y and D_z are not. Thus, if the angle of incidence is sufficiently large to induce a significant D_z, and hence E_z, in the antiferromagnet, we expect an overall power flow of density $E_z H_y$ parallel to the surface. At ω_T, this induces a large excitation (large B_y) and a significant absorption occurs. In s polarization, this mechanism is not possible if the substrate is highly metallic, since the only electric field component is along $\boldsymbol{y}$, and field continuity shorts out this component. This partially explains why the expected modes are not seen in figures 3(a) and 3(b). It is interesting, however, to observe that the argument

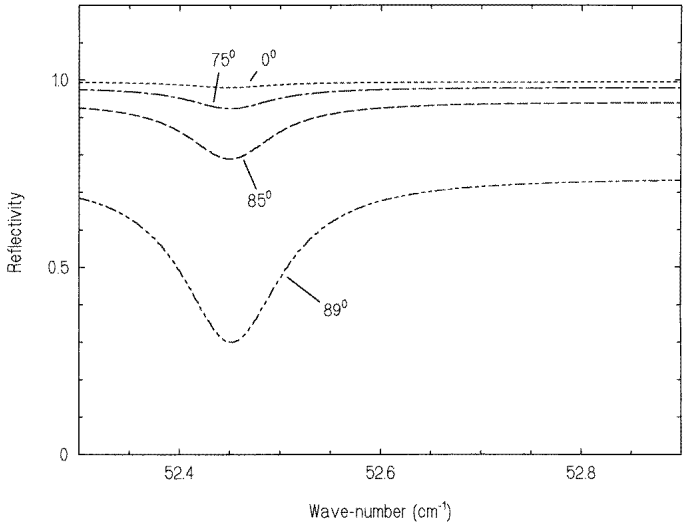

Figure 4. Calculated oblique-incidence reflectivity spectra, at various angles of incidence, in p polarization, for a structure consisting of 0.02 μm FeF_2 deposited on a metal with $\omega_p = 120\,000$ cm^{-1} and $\Gamma_p = 1000$ cm^{-1}. The FeF_2 anisotropy is along $\boldsymbol{x}$ or $\boldsymbol{z}$.

can still be used for a slightly metallic substrate, for which E_y is finite. In this case, it can be seen that continuity of B_z induces a large H_z at $\mu_{zz} = 0$, so, for anisotropy along $\boldsymbol{y}$, a weak dip at ω_L appears, in agreement with the result in figure 2(a).

It should be noted that, if the anisotropy is in-plane (along $\boldsymbol{x}$ in this case), the film thickness (0.02 μm) of the structure in figure 4 corresponds to only 43 lattice units. Strictly speaking, therefore, it is not correct simply to use the bulk permeability function represented by (1). Microscopic effects, mainly the pinning of magnon modes at the edges of the film, will result in a series of confined magnon modes, and the form of the permeability function should have a consequent change [22–24]. Thus it appears that there may be potential for experimental observation of thin-film confinement making use of the principles described above. We note that confinement effects have already been observed experimentally for much thicker (0.23 μm and 0.98 μm) MnF_2 films in transmission experiments [25].

Finally, it is worth commenting that, although the metal with $\omega_p = 150$ cm^{-1} and $\Gamma_p = 4$ cm^{-1} is mainly intended to be hypothetical, plasma frequencies and dampings of this order are found in practice in doped semiconductors [26–28]. An antiferromagnet deposited on such a semiconductor is therefore likely to display both s- and p-polarized surface modes in oblique-incidence reflectivity from vacuum.

5. Conclusions

We have predicted the existence of a new type of surface polariton at an antiferromagnet/metal interface. Surface polaritons of this type are somewhat similar to Berreman modes observed in alkali halide salts deposited on metal substrates. In particular it should be possible to observe them in simple oblique-incidence reflectivity. However, the modes have a number of unique features not present in the conventional Berreman effect, as listed below.

(1) Surface modes can appear in both s and p polarization. Nevertheless, if the metallic layer is a 'normal' metal, only p-polarized modes are likely to be observed.

(2) s-polarization dips occur in the region $\omega_T < \omega < \omega_L$, although p-polarization modes are not restricted to this range, and may, on occasions, occur slightly above ω_L. This contrasts with conventional Berreman dips which always occur at the LO phonon frequency (or slightly above it).

(3) The modes show a large shift with film thickness, whereas conventional Berreman dips show virtually no shift.

(4) For very thin films, the p-polarization modes occur at the transverse magnon frequency, whereas the conventional Berreman modes occur at the longitudinal phonon frequency.

We have demonstrated that, if the films are sufficiently thick, the frequencies of the spectral dips are well modelled by simple surface polariton theory. When the antiferromagnet film is thin, however, an alternative approach, based on the fields associated with reflection directly off the metal substrate, is more appropriate.

The modes should be especially important experimentally. In particular, we predict that their presence should serve as a useful tool in enhancing the signal in the far-infrared spectroscopy of thin-film structures of this nature.

Acknowledgments

The author has benefited from useful discussions with M C Oliveros, T J Parker, S R P Smith, R L Stamps and D R Tilley. This work was supported by the Brazilian agency CAPES.

References

[1] Cottam M G (ed) 1994 *Linear and Nonlinear Spin Waves in Magnetic Films and Superlattices* (Singapore: World Scientific)
[2] Ohlmann R C and Tinkham M 1961 *Phys. Rev.* **123** 425
[3] Sievers A J and Tinkham M 1963 *Phys. Rev.* **129** 1566
[4] Richards P L 1964 *J. Appl. Phys.* **35** 850
[5] Brown D E, Dumelow T, Parker T J, Abraha K and Tilley D R 1994 *Phys. Rev.* B **49** 12 266
[6] Abraha K, Brown D E, Dumelow T, Parker T J and Tilley D R 1994 *Phys. Rev.* B **50** 6808
[7] Jensen M R F, Parker T J, Abraha K and Tilley D R 1995 *Phys. Rev. Lett.* **75** 3756
[8] Lin X, Hadjipanayis G C and Shah S I 1994 *J. Appl. Phys.* **75** 6676
[9] Miller B H and Dahlberg E D 1996 *Appl. Phys. Lett.* **69** 3932
[10] Stamps R L, Camley R E and Hicken R J 1996 *Phys. Rev.* B **54** 4159
[11] Berreman D W 1963 *Phys. Rev.* **130** 2193
[12] Hoffmann F M 1983 *Surf. Sci. Rep.* **3** 107
[13] Chabal Y J 1988 *Surf. Sci. Rep.* **8** 211
[14] Gerbstein Yu M and Merlin D N 1974 *Fiz. Tverd. Tela* **16** 2584 (Engl. Transl. 1974 *Sov. Phys.–Solid State* **16** 1680)
[15] Dumelow T and Tilley D R 1993 *J. Opt. Soc. Am.* **10** 633
[16] Otto A 1968 *Z. Phys.* **216** 398
[17] Mills D L and Burstein E 1974 *Rep. Prog. Phys.* **37** 817
[18] Ashcroft N W and Mermin N D 1976 *Solid State Physics* (Philadelphia, PA: Saunders College)
[19] Dumelow T, Parker T J, Smith S R P and Tilley D R 1993 *Surf. Sci. Rep.* **17** 151
[20] Dumelow T and Camley R E 1996 *Phys. Rev.* B **54** 12 232
[21] White G K and Woods S B 1959 *Phil. Trans. R. Soc.* A **251** 273
[22] Orbuch R and Pincus P 1959 *Phys. Rev.* **113** 1213
[23] Stamps R L and Camley R E 1996 *Phys. Rev.* B **54** 15 200

[24] Dumelow T and Oliveros M C 1997 *Phys. Rev.* B **55** 994
[25] Lui M, Ramos C A, King A R and Jaccarino V 1990 *J. Appl. Phys.* **67** 5518
[26] Zawadzki W 1982 Mechanism of electron scattering in semiconductors *Band Theory and Transport Properties (Handbook on Semiconductors 1)* ed W Paul (Amsterdam: North-Holland) pp 713–803
[27] Romčević N, Popović Z V, Khokhlov D, Nikorich A V and König W 1991 *Phys. Rev.* B **43** 6712
[28] Perkowiz S 1993 *Optical Characterization of Semiconductors: Infrared, Raman, and Photoluminescence Spectroscopy* (London: Academic)